Impact of Physicochemical Properties of Biomass-based Fly Ash on Lignocellulose Removal from Pulping Spent Liquor

Germaine Cave and Pedram Fatehi *

A biomass-based fly ash was fractionated and ground to produce fly ash adsorbents of various compositions and particle sizes. It was determined that grinding had no noticeable impact on the surface area and micropore volume of the fly ash, but it increased the mesopore volume of the fly ash remarkably. Isotherm analysis on the lignin and chemical oxygen demand (COD) removals from a thermomechanical pulping (TMP) pressate (*i.e.*, spent liquor) was performed. It was determined that the adsorption process followed the Freundlich model, and the estimated maximum adsorption capacities for the lignin and COD on the fly ash were identified. The highest adsorption capacities for the COD and lignin were 204 mg fly ash/g TMP pressate and 149 mg fly ash/g TMP pressate, respectively, which were achieved under the treatment conditions of 298 K, 100 rpm when mixing the fly ash and pressate for 24 h. The potential impact of various physicochemical properties, such as the ionic strength and metals content of the fly ash, on the adsorption capacity for lignin and COD was also evaluated.

Keywords: Fly ash; Industrial processes; Adsorption; Lignin; Metal composition; Wastewater

*Contact information: Chemical Engineering Department, Lakehead University, 955 Oliver Road, Thunder Bay, ON, Canada, P7B5E1; *Corresponding author: pfatehi@lakeheadu.ca*

INTRODUCTION

In the thermomechanical pulping (TMP) process, wood chips are treated with steam or hot water prior to refining (Sixta 2006). The TMP process requires a substantial amount of water to treat wood chips. The most concentrated wastewater in the TMP process is the TMP pressate, which is the filtrate from the steam/hot water and/or primary refining stages (Zheng and Liao 2014). This spent liquor consists mostly of lignin and some wood extractives (Zasadowski *et al.* 2014) with a high chemical oxygen demand (COD) load (Sumathi and Hung 2004; Andersson *et al.* 2008). Various methods, such as advanced oxidation processes (AOPs), biological and electrochemical processes have been applied in pulp and paper wastewater treatment systems (Pérez *et al.* 2002; Jaafarzadeh *et al.* 2017a,b; Abedinzadeh *et al.* 2018). Generally, an activated sludge process is used to treat the produced spent liquor. However, the activated sludge system is sensitive to toxicity and shocking loads, and substances that are difficult to biodegrade can remain in the effluent after activated sludge treatment (Thompson *et al.* 2001). Moreover, treatment of this wastewater requires a large amount of land for operation and landfilling the sludge produced in the process (Thompson *et al.* 2001). In contrast, it has previously been stated that a combination of physicochemical and biological treatments could potentially offer a long-term solution for pulp and paper wastewater treatment operations (Pokhrel and Viraraghavan 2004). Furthermore, the use of an adsorption treatment has been considered

a suitable method for the removal of recalcitrant compounds, such as lignin, from pulp mill effluents (Pokhrel and Viraraghavan 2004; Sumathi and Hung 2004; Kamali and Khodaparast 2015).

In the pulping industry, a solid waste, such as biomass-based fly ash, is produced as a residue from burning wood residues and sludge. Canadian mills use approximately 22% of fly ash for beneficial purposes, such as composting, road construction, and soil conditioning, but the remainder of the ash is landfilled (Elliot and Mahmood 2006). The potential uses of biomass-based fly ash as an adsorbent for spent liquors from the pulping industry has been investigated in the past (Wang and Wu 2006; Gupta *et al.* 2009; Cretescu *et al.* 2015; Lanzerstorfer 2015; Singh and Prasad 2015). Lignin removal from a TMP pressate with a biomass-based fly ash has been studied as well (Oveissi and Fatehi 2015a). It has been observed that 53% of lignin was removed *via* mixing biomass-based fly ash with a TMP pressate under the conditions of 55 mg fly ash/g TMP pressate, 303 K, and 3 h (Oveissi and Fatehi 2015a). Other researchers have studied the adsorption of lignin on a biomass-based fly ash from a model solution (Andersson *et al.* 2011) and TMP bleaching effluent (Andersson *et al.* 2012). The compositions are expected to differ for various industrially produced effluents. Therefore, the results available in the literature may not be reliable for predicting the adsorption of TMP pressate components on a biomass-based fly ash. Although experimental results have supported the adsorption of lignocelluloses onto fly ash, no study has been conducted to relate the properties of biomass-based fly ash with its adsorption performance. To implement the use of fly ash as an adsorbent in various industries, such a correlation should be developed.

It is well known that the characteristics of the adsorbents impact their adsorption performance (Faust and Aly 1998). It has previously been reported that, for nonporous adsorbents, particle size reduction increased the adsorption capacity, which was attributed to the considerably increased surface area and possible exposure of more accessible sites for adsorption (Faust and Aly 1998). However, the particle size reduction of a highly porous adsorbent seemed to have a limited impact on its surface area or adsorption capacity because small molecules (*e.g.*, phenols) would have access to the surface area inside pores, and the particle size would have a more limiting effect on the adsorption (Faust and Aly 1998). One objective of this study was to determine how the particle size of a biomass-based fly ash impacts its adsorption performance for lignocelluloses from a TMP pressate.

In contrast to activated carbon, which is mainly composed of organic compounds, fly ash consists of organic and inorganic elements. While organic compounds may facilitate the development of hydrogen bonding with the lignocelluloses in a pressate, the inorganic compounds may help with the charge interaction and hydrophobic-hydrophobic interaction with lignocelluloses. The inorganic compounds may also facilitate the complexation of lignocelluloses in a pressate. Although the adsorption of lignocelluloses onto activated carbon has been studied comprehensively, the impact of the physicochemical properties of fly ash on its adsorption performance is unclear. Knowledge concerning such impacts is essential for the development of fly ash-based adsorption processes to treat pressate. This is because these characteristics may vary with time and influence the efficiency of the adsorption process. To have a consistent adsorption performance in industry settings, information should be available to both understand the contribution of different characteristics of fly ash on its adsorption capacity and minimize the variation in the adsorption efficiency. The purpose of this study was to characterize the biomass-based fly ash and relate its properties to its adsorption performance for the components of a TMP pressate. In a series of experiments, fly ash samples with different particle sizes and

chemical compositions were made, and the effects of these parameters on the adsorption performance of the fly ash was investigated.

Particle size reduction can be performed *via* mechanical grinding and fractionation of the fly ash. Despite their popularity, it is unclear which process would be more reliable for producing fly ash with the desired properties. Therefore, another objective of this work was to study the impact of these procedures on producing fly ash with a high adsorption performance. An isotherm analysis was also conducted on the fly ash samples using the Freundlich and Langmuir models to describe the changes in the chemical oxygen demand (COD) and lignin of a TMP pressate. Also, the relationship between the physicochemical properties of the fly ash samples and their performance as an adsorbent was established. This paper contributes to the development of biomass-based fly ash adsorption systems to treat wastewater effluents.

EXPERIMENTAL

Materials

Biomass-based fly ash and TMP pressate samples were obtained from a pulp mill located in central Canada. This fly ash was produced *via* burning tree branches, sludge, and saw dust in a pulp mill boiler. The fly ash was dried overnight in an oven at 378 K and stored in plastic bags at room temperature prior to use. The TMP pressate was stored in a refrigerator at 277 K prior to use. Sodium hydroxide (98 wt.%), hydrochloric acid (37 wt.%), sulfuric acid (95 wt.%), sodium chloride, calcium chloride, and potassium chloride were purchased from Sigma Aldrich (St. Louis, MO, USA). The COD kit (K-7365) was obtained from CHEMetrics Inc. (Midland, MI, USA).

Methods

Fractionation of the biomass-based fly ash

The fly ash was mechanically sieved based on the method described by Zhu *et al.* (2013). In this method, ASTM E11 sieves were used in conjunction with a Meinzer II Sieve Shaker (CSC Scientific, Fairfax, VA, USA), and fractionation was performed in 10 min intervals with 200 g of fly ash at a time. A sample of the fly ash was prepared by sieving with 10 and 400 meshes, and the fly ash retained on the 400 mesh was mixed well and labelled S_0. The fly ash fraction that was retained on the 10 mesh was discarded, as an initial assessment showed this fraction has a limited adsorption capacity. Two sets of experiments were conducted to produce fly ash samples with certain specifications. Illustrations of the fractionation and grinding procedure used on the fly ash samples are given in Figs. 1 and 2.

To produce fly ash with similar particle sizes and different elemental compositions, the collected fly ash sample was fractionated with 16, 20, 40, 60, 140, 200, and 400 meshes. These samples had particle size ranges of 0.037 mm to 0.074 mm, 0.105 mm to 0.250 mm, 0.250 mm to 0.420 mm, 0.420 mm to 0.841 mm, and 1.19 mm to 2.00 mm; and they were labeled F_01, F_02, F_03, F_04, and F_05, respectively. The surface areas and pore volumes of the fly ash samples were determined. The sieved fly ash samples (F_01, F_02, F_03, F_04, and F_05) were ground separately for 20 s to 30 s using a grinder (Bel-Art SP Scienceware micro-mill, Wayne, USA). The samples were then sieved again with 200 and 400 meshes. The fly ashes retained on the 400 mesh were collected and labelled as F1, F2, F3, F4, and F5, respectively, and had the same particle size range of 0.037 mm to 0.074 mm. This

fractionation exercise was to ensure the collection of fly ash samples with similar sizes. The surface area, pore volume, and carbon and metals contents of the ground fly ash samples were then analyzed. The S_0 fly ash sample that was set aside was also ground and sieved prior to use as described for the fly ash samples above, yielding a fly ash sample (S) with a particle size range of 0.037 to 0.074 mm.

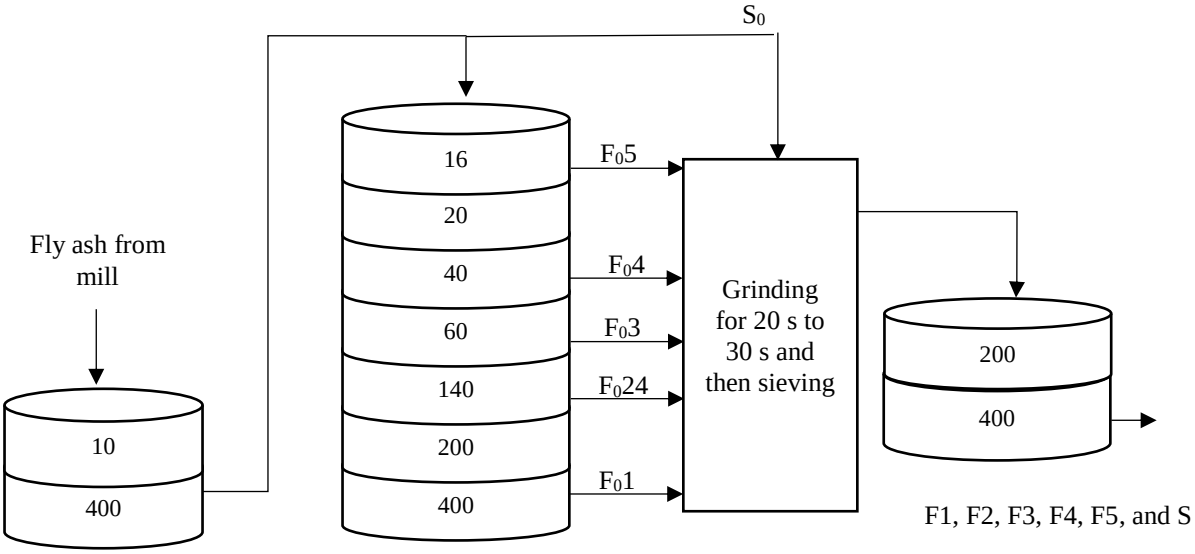

Fig. 1. Procedure for the fractionation and grinding of the fly ash to produce samples with different compositions and similar particles sizes (F1, F2, F3, F4, and F5)

To produce fly ash samples with similar compositions and different particle sizes, a portion of F_04 was ground for 10 s to 15 s using a grinder (Bel-Art SP Scienceware micro-mill). The ground F_04 was then fractionated using sieves with 50, 60, 100, and 140 mesh sizes. The fly ash fractions that were retained on the sieves of the 50 and 100 meshes were discarded, as these samples had particle size ranges that overlapped with those of the other samples. The fly ash retained on the sieves with 140 and 60 meshes were labeled as F4S and F4M, respectively, and their surface area and pore volume were characterized. These samples had particle size ranges of 0.105 mm to 0.149 mm and 0.250 mm to 0.297 mm, respectively.

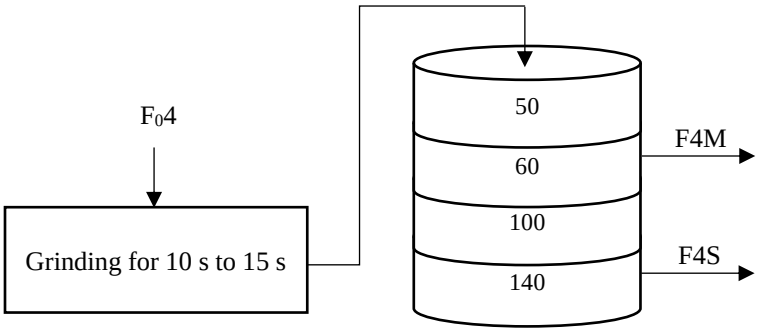

Fig. 2. Procedure for the grinding and fractionation of the fly ash to produce fly ash samples with similar compositions and different sizes (F4M and F4S)

Characterization of the biomass-based fly ash

In this set of experiments, 0.2-g fly ash samples were analyzed with a Vario EL cube elemental analyzer (Elementar, Langenselbold, Germany) to determine the carbon content, as was described by Fadeeva *et al.* (2008). The metals content of the fly ash samples was analyzed by inductively coupled plasma-optical emission spectrometry (ICP-OES) using a Varian Vista Pro (Varian Inc., Palo Alto, CA, USA) with a CETAC ASX-510 autosampler (Teledyne CETAC Technologies, Omaha, NE, USA) based on the EPA 3051A method (Cave and Fatehi 2017). In this method, 0.2-g fly ash samples were digested with aqua regia (*i.e.*, a 1:3 molar ratio of nitric acid and hydrochloric acid) in a Mars Xpress microwave using an Xpress closed vessel (CEM Corporation, Matthews, USA). The digestion conditions involved a ramp time of 20 min to a temperature of 448 K, which was then maintained for 25 min. After completion, the samples were cooled and diluted with 40 mL of deionized water prior to the ICP-OES analysis.

The surface area of the fly ash samples was measured with a NOVA-2200e surface area analyzer (Quantachrome Instruments, Boynton Beach, FL, USA) based on the method previously described by Wang *et al.* (2006), and by applying the Brunauer-Emmett-Teller (BET) theory. The fly ash samples were dried overnight at 403 K, and 0.05 g of the fly ash samples were then degassed at 523 K for 4 h prior to analysis. The isotherms were determined between the relative pressure range of 0.01 and 0.99 at a temperature of 77 K. The BET surface area was determined with the multipoint method by fitting the data from the nitrogen adsorption isotherms between the relative pressures of 0.05 and 0.3. The total pore volumes were determined using the NovaWin software (version 11.0, Quantachrome Instruments). The micropore volume of the fly ash samples was calculated by fitting the data from the nitrogen adsorption isotherms between the relative pressure range of 0.06 and 0.2 to the Dubinin-Radushkevich equation (Hsieh and Teng 2000; Scherdel *et al.* 2010). The mesopore volume was then estimated by subtracting the micropore volume from the total pore volume (Hsieh and Teng 2000; Yang *et al.* 2010).

To determine the solubility and soluble components of the fly ash samples, fly ash samples were added to 50 g of deionized water in 250 mL Erlenmeyer flasks at a dosage of 70 mg/g fly ash/water and the flasks were sealed. The mixtures were then shaken at 100 rpm in a Boekel water bath shaker at 298 K for 2 h. The mixtures were filtered with a glass filter apparatus (Millipore) and filter paper (Whatman No. 1) and the fly ash leachate was collected. The metal content of the leachate samples was then analyzed by ICP-OES. Then, the leachate was dried in an oven at 378 K, and the solubility was determined based on Eq.1:

$$\text{Solubility (wt.\%)} = \frac{Mass\ of\ dissolved\ components\ in\ leachate}{Initial\ mass\ of\ fly\ ash} \times 100 \qquad (1)$$

Kinetic studies

The biomass fly ash sample, S with a particle size range of 0.037 to 0.074 mm was added to 50 g of TMP pressate in 250 mL Erlenmeyer flasks at a dosage of 15 mg/g fly ash/TMP pressate. The pH of the mixture was then adjusted to 6, and the flasks were sealed. The samples were then shaken at 100 rpm in a Boekel water bath shaker at 298 K for various time intervals of 0.5 h, 1 h, 2 h, 3 h, 4 h, 5 h, 6 h, 12 h, or 24 h for determining the equilibrium time. The samples were filtered with a glass filter apparatus (Millipore) and filter paper (Whatman No. 1) after the adsorption treatment, and the filtrates were collected for COD, lignin, and pH analyses. All adsorptions tests were repeated, and the average results were reported.

Adsorption isotherm studies

The fly ash samples F1, F2, F3, F4, F5, F4S, F4M, and $F_0$4 were added to 50 g of TMP pressate in 250-mL Erlenmeyer flasks at various dosages ranging from 5 mg fly ash/g TMP pressate to 100 mg fly ash/g TMP pressate. The pH of the mixtures was adjusted to 6 (i.e., the original pH value of TMP pressate), and the flasks were sealed. The samples were then shaken at 100 rpm in a Boekel water bath shaker (Feasterville, PA, USA) and 298 K for 24 h. The samples were then filtered with a glass filter apparatus (Millipore, Burlington, MA, USA) using Whatman No. 1 filter papers (Sigma Aldrich, St. Louis, MO, USA), and the filtrates were collected for the COD and lignin analyses. All of the adsorption tests were repeated, and the average results were reported.

COD and lignin adsorption calculations

The COD and lignin removals were determined using Eq. 2, and the amounts of COD removed from the TMP pressate and lignin adsorbed on the fly ash per unit mass of fly ash at equilibrium conditions, q_e (mg/g) were determined using Eq. 3,

$$Removal\ \% = \frac{C_0 - C_F}{C_0} \times 100 \quad (2)$$

$$q_e = \frac{(C_0 - C_e)}{m} V \quad (3)$$

where m refers to the mass of the fly ash (g), V is the volume of the TMP pressate (L), C_0 is the COD or lignin concentration in the filtrate of the control samples (mg/L), and C_F and C_e refer to the COD and lignin concentrations (mg/L) in the filtrate after the fly ash adsorption treatments, respectively.

The concentration of the filtrates in the control samples was used to account for the effect of filtration on the concentration (*i.e.*, no addition of fly ash). In this set of experiments, a portion of the TMP pressate was filtered initially with a glass filter apparatus (Millipore) and Whatman No. 1 filter papers. Afterwards, the filtrates were collected for the COD and lignin analyses.

Model analysis

The data from the isotherm experiments was analyzed by regression analysis of the linearized forms of the Freundlich and Langmuir models. The Freundlich equation and its linearized form used in this study are given as Eqs. 4 and 5, respectively,

$$q_e = K_F C_e^{1/n} \quad (4)$$

$$\ln q_e = \frac{1}{n} \ln C_e + \ln K_F \quad (5)$$

where K_F is the Freundlich constant ($mg^{1-(1/n)}\ L^{(1/n)}$ /g), which is the relative adsorption capacity of the adsorbent, and n is a unitless constant that indicates the favorability of adsorption.

The maximum adsorption capacity (q_m, mg/g) was estimated using Eq. 6 by performing the isotherm tests experimentally with a constant initial concentration and varying the dosage of the adsorbent (Hamdaoui and Naffrechoux 2007):

$$q_m = K_F C_0^{1/n} \quad (6)$$

The Langmuir equation and its linearized form used in this study are given as Eqs. 7 and 8, respectively:

$$q_e = \frac{q_m b C_e}{1 + b C_e} \quad (7)$$

$$\frac{C_e}{q_e} = \frac{1}{q_m} C_e + \frac{1}{q_m b} \quad (8)$$

where b is a constant that is related to the affinity between the adsorbent and adsorbate (L/mg).

COD, lignin, hemicellulose and turbidity analyses

The COD analysis was performed according to the spectrophotometric method using a Genesys 10S ultraviolet-visible (UV-Vis) spectrophotometer (Thermo Fisher Scientific, Waltham, USA) at 620 nm. In this method, 2 mL of the samples were added to COD vials (CHEMetrics Inc.) and incubated in a CR 2200 thermoreactor (WTW, Weilheim, Germany) for 2 h at 423 K prior to measuring the COD with the spectrophotometer. The lignin concentration was determined by the spectrophotometric method described previously by Liu *et al.* (2011) using the Genesys 10S UV-Vis spectrophotometer at 205 nm (Saeed *et al.* 2012a). The pH of the samples was adjusted to 7 (± 0.25) with 0.1 M NaOH or 0.1 M HCl prior to the UV analysis.

The TMP pressate was treated with 4 wt.% sulfuric acid at 121 ºC for 1 h in an oil bath so that hemicellulose (oligomeric sugars) were converted to monomeric sugars. The acidulated samples were then filtrated by 0.20 µm membrane and then measured by a Dionex CarboPacTM ICS-5000 ion chromatography unit equipped with CarboPacTM SA10 column (Dionex Co., Canada) and Thermo Scientific electrochemical detector. Deionized water (with a 1.2 mL/min flow rate) and KOH (1 mM) generated by an eluent generator (EGC 500 KOH) (1 mL/min flow rate) were used as flow phase and eluent, respectively. The turbidity of TMP pressate was identified by 2100AN turbidimeter (Hach Co., CO, USA).

Hydrodynamic diameter analysis

In this set of experiments, lignin was separated from the TMP pressate *via* acidification based on the method described in the literature (Liu *et al.* 2011; Oveissi and Fatehi 2015b). Initially, the TMP pressate was centrifuged at 1000 rpm for 10 min using a Sorvall ST 16 centrifuge (Thermo Fisher Scientific) to remove undissolved particles. The filtrate was then acidified with sulfuric acid (60 wt.%) so that the pH was 1.5, and then the solution was shaken at 100 rpm in the water bath shaker at 298 K for 1 h. After acidification, the sample was centrifuged at 3000 rpm for 15 min, and the lignin precipitate was then collected. The precipitate was suspended in deionized water and neutralized (pH = 7). The lignin solution containing the precipitate was then dried to a constant weight in an oven at 333 K. Then, a 1-wt.% lignin solution was prepared in deionized water. The solution was stirred overnight, and the hydrodynamic diameter of the lignin was measured by dynamic light scattering with a BI2000 (Brookhaven Instrument Corporation, Holtsville, USA) at a scattering angle of 90°, as was described by Li *et al.* (2006).

Zeta potential

The zeta potential of F1 and F4 in the TMP pressate at different concentrations of sodium chloride was determined using a NanoBrook ZetaPALS potential analyzer (Brookhaven Instrument Corporation). In this method, F1 or F4 was added to 50 g of TMP pressate in 250-mL Erlenmeyer flasks at a dosage of 70 mg fly ash/g TMP pressate, and the pH of the mixture was adjusted to 6. Next, the mixtures were adjusted to various sodium

chloride concentrations ranging from 0.04 M to 0.5 M using a 2 M sodium chloride solution, and the flasks were sealed. The samples were then shaken at 100 rpm in the water bath shaker at 298 K for 24 h. Then, 0.5 mL of the unfiltered samples were diluted in 20 mL of 1 M potassium chloride solution and their electrophoretic mobility was determined in triplicate using the NanoBrook ZetaPALS potential analyzer at 298 K, and the average results were reported. The zeta potential was then calculated by the software using the Smoluchowski model.

Coagulation experiments

The coagulation experiments were performed using a focused beam reflectance measurement (FBRM) instrument and Particle Track E25 probe (Mettler-Toledo AutoChem) by monitoring chord length of the colloids in the solutions as described previously (Fatehi *et al.* 2016). In one set of experiments, the FBRM probe was immersed 20 mm below the solution level of 200 g samples of a TMP pressate in 400 mL glass beakers, and the TMP pressate was stirred at 200 rpm until steady state conditions were achieved. Then, various coagulant solution dosages of potassium chloride (546 to 4567 mg/kg KCl/TMP pressate) and calcium chloride (1040 to 2770 mg/kg $CaCl_2$/TMP pressate were added separately at pH 6. The experiments were then repeated and the average results were reported. The coagulation efficiency of the coagulants studied was monitored by FBRM via quantifying the mean chord length and chord length distribution of particles produced in the samples after 30 min at 298 K. After the coagulation experiments, all the samples were filtered with a glass filter apparatus (Millipore) and filter paper (Whatman No. 1), and the filtrates were collected for COD and lignin analyses. The COD and lignin removals were determined using Eq. 2.

RESULTS AND DISCUSSION

Characterization of the TMP Pressate

The original TMP pressate contained 2.2 g/L lignin, 0.7 g/L hemicellulose, 2912 mg/L COD, and 637 NTU turbidity, and had a pH of 6.1. Oveissi and Fatehi (2015a) reported that a TMP pressate contained 4.5 g/L lignin, 0.7 g/L hemicellulose, 5311 mg/L COD, and 486 NTU turbidity, and had a pH of 5.3. These results suggested that the TMP pressate used in this study represented a medium-strength pressate compared with previous studies (Zasadowski *et al.* 2014; Oveissi and Fatehi 2015a). Furthermore, the hydrodynamic diameter of the lignin present in the TMP pressate was determined to be 8.5 nm. Oveissi and Fatehi (2015b) reported the lignin present in a hydrolysis liquor to have a hydrodynamic diameter of 2.1 nm.

Characteristics of the Biomass-based Fly Ash

The elemental components of the fly ash samples F1, F2, F3, F4, and F5 are given in Table 1. As these samples were the ground versions of samples $F_0$1, $F_0$2, $F_0$3, $F_0$4, and $F_0$5, it could be claimed that the ground and unground samples had the same compositions. It was observed that as the particle size of the fly ash samples decreased, their carbon content decreased, while their metals contents increased. Similar results have been reported previously for a biomass-based fly ash (Girón *et al.* 2013). The carbon content of the fly ashes will be reduced by an efficient burning of biomass in the furnace (Rajamma *et al.* 2009). The high carbon content of larger particles might result from the unburned portion

of wood chips and tree branches. All residual incinerated inorganic elements were left as ash and salts with smaller particle sizes. In our previous study, X-ray diffraction crystallography (XRD) spectra also confirmed that different crystalline phases were present in the different fraction of fly ash samples (Cave and Fatehi 2017). With a particle size of 0.037 to 0.250 mm, lime (CaO), anhydrite ($CaSO_4$), portlandite ($Ca(OH)_2$) and calcite ($CaCO_3$) were present. Anhydrite, calcite, and portlandite were the three crystalline phases present in the fraction of 0.250 to 0.841 mm. In the large fraction of 0.841 to 2.00 mm, calcite was the only crystalline phase identified (Cave and Fatehi 2017).

Table 2 lists the elemental compositions of the biomass-based fly ash samples (F4, F4S, F4M, and F_04). The results confirmed that these fly ash samples had similar chemical compositions, but they had slightly different calcium contents. Also, these samples had different particle sizes.

Table 1. Elemental Compositions of the Ground and Unground Samples

Element	F1, F_01	F2, F_02	F3, F_03	F4, F_04	F5, F_05
	wt.%				
Carbon	27.14	37.19	42.37	75.04	82.65
Aluminum	0.99	1.43	0.72	0.94	0.11
Barium	0.15	0.15	0.13	0.03	0.05
Calcium	19.68	15.42	16.57	2.76	3.40
Iron	0.63	1.08	0.48	0.76	0.06
Potassium	4.03	3.33	3.70	1.12	0.77
Magnesium	1.54	1.50	1.32	0.40	0.27
Manganese	0.81	0.67	0.74	0.13	0.15
Sodium	0.96	0.65	0.66	0.31	0.15
Zinc	0.20	0.16	0.18	0.02	0.01
Other	43.88	38.43	33.13	18.49	12.38

Table 2. Elemental Compositions of the Ground F4, F4S, F4M, and F_04

Element	F4	F4S	F4M	F_04
	Particle Size Range (mm)			
	0.037 to 0.074	0.105 to 0.149	0.250 to 0.297	0.420 to 0.841
	wt.%			
Carbon	75.04	73.11	72.00	73.16
Aluminum	0.94	1.19	0.91	1.09
Barium	0.03	0.03	0.03	0.04
Calcium	2.76	2.53	2.54	3.36
Iron	0.76	0.92	0.68	0.81
Potassium	1.12	1.00	0.93	1.11
Magnesium	0.40	0.50	0.46	0.51
Manganese	0.13	0.11	0.11	0.15
Sodium	0.31	0.45	0.34	0.41
Zinc	0.02	0.02	0.01	0.02
Other	18.49	20.15	20.15	19.35

The surface area and pore volumes of the fractionated fly ash samples ($F_0$1, $F_0$2, $F_0$3, $F_0$4, and $F_0$5) and ground fly ash samples (F1, F2, F3, F4, F5, F4S, and F4M) were determined, and the results are given in Table 3.

Table 3. Characteristics of the Fractionated Biomass-based Fly Ash Samples

Parameter	$F_0$1	$F_0$2	$F_0$3	$F_0$4	$F_0$5
	Particle Size Range (mm)				
	0.037 to 0.074	0.105 to 0.250	0.250 to 0.420	0.420 to 0.841	1.19 to 2.00
Surface Area (m^2/g)	105.0	150.0	193.0	387.0	465.6
V_{total} (cm^3/g)	0.077	0.106	0.126	0.240	0.269
V_{micro} (cm^3/g)	0.053	0.074	0.093	0.203	0.238
V_{meso} (cm^3/g)	0.024	0.032	0.033	0.037	0.031
	F1	F2	F3	F4	F5
	Particle Size Range (mm)				
	0.037 to 0.074	0.037 to 0.074	0.037 to 0.074	0.037 to 0.074	0.037 to 0.074
Surface Area (m^2/g)	109.0	144.9	189.8	393.4	471.9
V_{total} (cm^3/g)	0.094	0.118	0.139	0.239	0.287
V_{micro} (cm^3/g)	0.054	0.072	0.095	0.200	0.245
V_{meso} (cm^3/g)	0.040	0.046	0.044	0.039	0.042
	F4	F4S	F4M	$F_0$4	
	Particle Size Range (mm)				
	0.037 to 0.074	0.105 to 0.149	0.250 to 0.297	0.420 to 0.841	-
Surface Area (m^2/g)	393.4	318.4	440.9	387.0	-
V_{total} (cm^3/g)	0.239	0.203	0.268	0.240	-
V_{micro} (cm^3/g)	0.200	0.164	0.228	0.203	-
V_{meso} (cm^3/g)	0.039	0.039	0.040	0.037	-

V_{total} = total pore volume
V_{micro} = micropore volume determined by Dubinin-Radsukevich analysis
V_{meso} = mesopore volume (total pore volume - micropore volume)

The surface area ranged from 105.0 m^2/g to 471.9 m^2/g, the total pore volume ranged from 0.077 cm^3/g to 0.287 cm^3/g, and the micropore volume ranged from 0.053 cm^3/g to 0.245 cm^3/g. Also, the surface area, total pore volume, and micropore volume increased as the particle size increased before grinding (*i.e.*, $F_0$1, $F_0$2, $F_0$3, $F_0$4, and $F_0$5); the surface areas and micropore volumes of the samples did not change remarkably after grinding (*i.e.*, for F1, F2, F3, F4, and F5). The mesopore volumes of the fly ash samples were fairly similar for $F_0$1 through $F_0$5 (approximately 0.031 cm^3/g), as well as for samples F1 through F5 (approximately 0.042 cm^3/g). The results also indicated that grinding of the fly ash samples increased their mesopore volume, as the shielded internal pores became available and total pore volume increased (Table 3). Thus, the increase in the mesopore volume was very limited, and the relative increase in the surface area was affected much less than the relative

increase in the pore volume, leading to insignificant changes in surface area of fly ash. The results in Tables 1 and 3 also indicated that the surface area and micropore volume increased as the carbon content increased. As the carbon content of the fly ash originated from unburned biomass, the increase in the carbon content was associated with the increase in the surface area and micropore volume because biomass is a porous material (Kao *et al.* 2000; Wang *et al.* 2005).

It was also observable that the surface areas, total pore volumes, and micropore volumes of F4, F4S, F4M, and $F_0$4 were different, but their chemical compositions were similar (Table 2). Moreover, the mesopore volumes of F4, F4S, F4M, and $F_0$4 were similar (approximately 0.039 cm^3/g).

Determination of the equilibrium time

Figure 3 shows the equilibrium time for lignin adsorption and COD removal from a TMP pressate by sample (S). The equilibrium time for lignin adsorption was attained at approximately 6 h, and the amount of lignin adsorbed from a TMP pressate on sample (S) was 89.1 mg/g. In the study by Andersson *et al.* (2012), the equilibrium time for adsorption of lignin on a biomass fly ash was reported to be 6 h, and thus the results are consistent with the literature results. The equilibrium time for the COD removal was reached at approximately 2 h and the adsorption of components contributing to COD on S was 74.1 mg/g under the conditions studied. The results also indicate that approximately 89 % of the lignin and COD removals occurred within 1 h of the adsorption treatment.

It was assumed that the equilibrium time for sample (S) would be representative of the individual fly ash samples. All biomass fly ash samples were obtained originally from S_0 and the potential impact of grinding on the equilibrium time may be representative by sample (S). However, the individual fly ash samples may reach equilibrium conditions at different times. To ensure that the isotherm studies were conducted under equilibrium conditions an equilibrium time of 24 h was used in this study for all isotherm tests. In one study on the removal of phenolic and lignin compounds from a bleached kraft mill by fly ash, the equilibrium time was observed to occur after 1 h and isotherm studies were conducted for 24 h (Ugurlu *et al.* 2005). Furthermore, the results in Fig. 3 indicate that the equilibrium conditions were maintained at 24 h, and thus isotherm tests were assumed to be conducted under equilibrium conditions.

Isotherm Analysis

The adsorption isotherm studies were conducted using the Freundlich and Langmuir models, as they are frequently used for modeling adsorption processes (Foo and Hameed 2010). The data on the lignin and COD removals from the TMP pressate on the biomass-based fly ash samples F1, F2, F3, F4, F5, F4S, F4M, and $F_0$4 was fitted to the isotherm models (figures not shown). The resulting Freundlich and Langmuir parameters are given in Table 4 for F1, F2, F3, F4, and F5, and are given in Table 5 for F4, F4S, F4M, and $F_0$4.

For the lignin adsorption, the Freundlich equation and Langmuir equation yielded R^2 values of 0.951 to 0.993 and 0.897 to 0.985. For the COD removal, the R^2 values of Freundlich equation was calculated to be 0.964 - 0.995, while the Langmuir equation yielded unsatisfied R^2 values of 0.121 to 0.786.

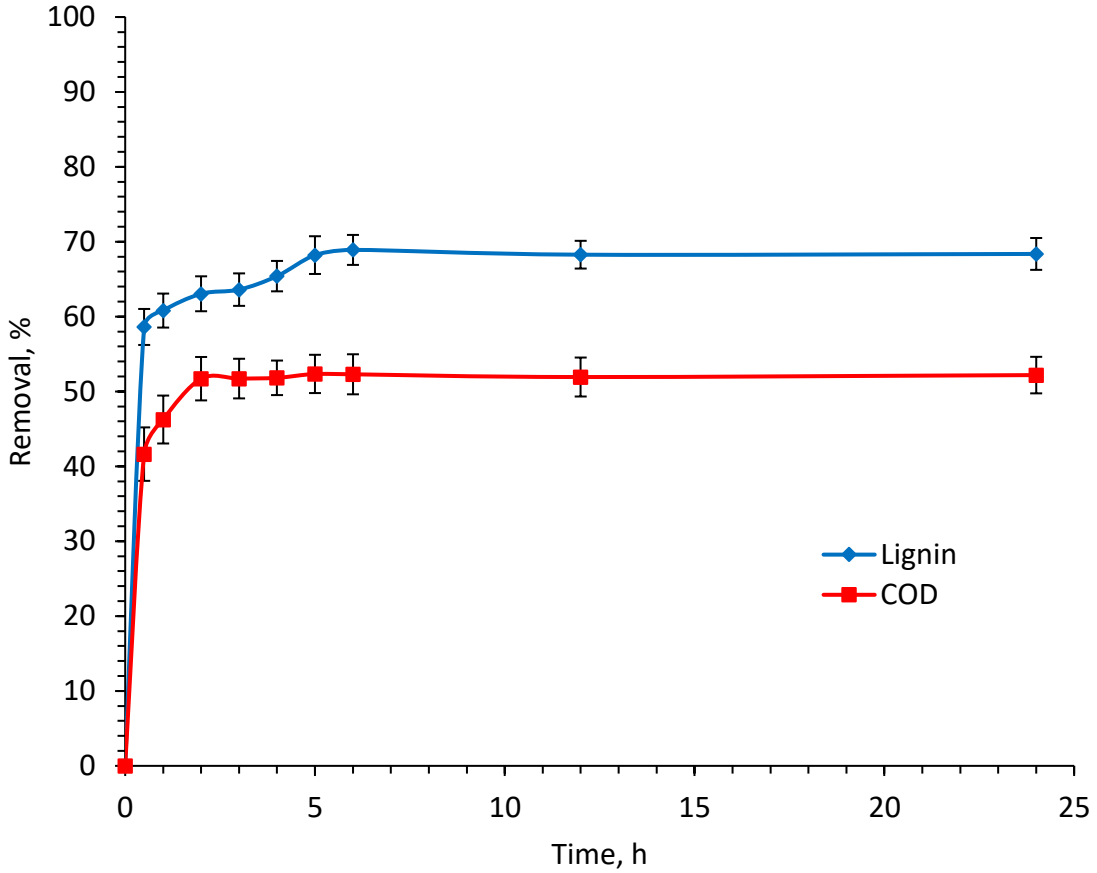

Fig. 3. Removals of lignin and COD from a TMP pressate by S as a function of adsorption time. The adsorption conditions were 15 mg/g fly ash/TMP pressate; pH of 6; 100 rpm agitation speed; and 298 K. The fly ash samples had a particle size range of 0.037-0.074 mm.

Overall, the results indicated that the both Freundlich and Langmuir equations appear to produce reasonable models of lignin adsorption (Mall *et al.* 2005), suggesting that further experiments are needed to provide more data for the determination of more suitable model describing lignin adsorption processes. The COD adsorption systems were best described by linear Freundlich equation, suggesting nonideal multilayer adsorption of COD contributing compounds on fly ash surfaces (Gupta *et al.* 2007). Furthermore, because the *n* values were greater than one, the COD adsorption from the TMP pressate was favorable (Tables 4 and 5).

Impact of the Ionic Strength

The solubility of fly ash was determined to be 8.81 %. The soluble components in the biomass fly ash leachate were measured. Under the conditions of 70 mg/g fly ash/water, 100 rpm and 298 K for 2 h leaching treatment, the main metals that were detected in the biomass leachate were Ca (1218.7 mg/L), K (2415.8 mg/L) and Na (464.8 mg/L). The trace metals that were detected to a significant extent were Ba, Mg, Mn, Si, Sr, and Zn and the remaining trace metals had a concentration of less than 0.1 mg/L or were below their minimum detection limit.

Table 4. Parameters of the Freundlich and Langmuir Isotherms for Lignin and COD Removal in a TMP Pressate by F1, F2, F3, F4, and F5

Parameter	F1	F2	F3	F4	F5
	Lignin				
Freundlich					
n	2.02	1.92	1.93	1.72	1.67
K_F ($mg^{1-(1/n)}$ $L^{(1/n)}$/g)	3.49	2.77	2.83	1.31	1.34
q_m (mg/g)	149	142	143	106	125
R^2	0.987	0.979	0.993	0.986	0.981
Langmuir					
b (L/mg)	2.29E-03	1.92E-03	2.00E-03	1.09E-03	1.69E-03
q_m (mg/g)	161	159	157	143	132
R^2	0.918	0.916	0.939	0.922	0.906
	COD				
Freundlich					
n	1.36	1.23	1.23	1.10	1.20
K_F ($mg^{1-(1/n)}$ $L^{(1/n)}$/g)	0.57	0.33	0.41	0.15	0.12
q_m (mg/g)	161	168	204	156	70
R^2	0.990	0.991	0.988	0.995	0.964
Langmuir					
b (L/mg)	4.67E-04	3.03E-04	3.25E-04	1.25E-04	1.80E-04
q_m (mg/g)	300	399	464	711	248
R^2	0.786	0.768	0.665	0.617	0.318

pH = 6

The addition of biomass-based fly ash to the TMP pressate increased the pH of the solution, which was caused by the high metal oxide content (*e.g.*, CaO) of fly ash, which could easily be hydrolyzed in the form of metal ions and hydroxyl ion (Duan and Gregory 2003). For a fly ash dosage of 70 mg fly ash/g TMP pressate, the pH values of the resulting mixtures with F1, F2, F3, F4, and F5 were 12.7, 12.6, 12.5, 9.8, and 9.9, respectively. According to Table 2, the higher pH values corresponded to a higher calcium content. The pH at point of zero charge (pHpzc) of fly ash was found to be approximately 6.5. The number of negative charges on the surface of fly ash was expected to increase at a pH above pH_{PZC} leading to electrostatic repulsion between lignin's hydroxyl groups and adsorbent. It was reported in our previous study that pH adjustment had a significant effect on the treatment of TMP pressate by fly ash (Cave and Fatehi 2017). The removal of lignin from the TMP pressate at an acidic pH was enhanced as lignin is generally less soluble under acidic conditions due to protonation of its carboxylate and phenolate groups. Therefore, different dosages of hydrochloric acid were required to adjust the pH of the systems to 6, which is below pHpzc and consistent with the original pH value of TMP pressate.

Table 5. Parameters of the Freundlich and Langmuir Isotherms for the Lignin and COD Removal in the TMP Pressate by F4, F4S, F4M, and $F_0$4

Parameter	F4	F4S	F4M	$F_0$4
	Particle Size Range (mm)			
	0.037 to 0.074	0.105 to 0.149	0.250 to 0.297	0.420 to 0.841
	Lignin			
Freundlich				
n	1.66	1.98	2.15	1.43
K_F ($mg^{1-(1/n)}$ $L^{(1/n)}$/g)	2.82	3.80	3.68	1.15
q_m (mg/g)	270	175	124	230
R^2	0.951	0.964	0.974	0.969
Langmuir				
b (L/mg)	2.47E-03	2.94E-03	2.37E-03	1.64E-03
q_m (mg/g)	233	165	136	204
R^2	0.985	0.975	0.923	0.897
	COD			
Freundlich				
n	1.04	1.04	1.09	1.14
K_F ($mg^{1-(1/n)}$ $L^{(1/n)}$/g)	0.11	0.07	0.06	0.12
q_m (mg/g)	170	116	64	103
R^2	0.986	0.994	0.969	0.985
Langmuir				
b (L/mg)	6.49E-05	4.60E-05	5.80E-05	1.60E-04
q_m (mg/g)	1347	1272	580	387
R^2	0.170	0.254	0.121	0.401

The pH adjustment step might change the ionic strength of the TMP pressate *via* the addition of hydrochloric acid. To investigate the impact of the ionic strength on the zeta potential of the pressate, different NaCl concentrations (0.5 M to 9 M) were prepared in the TMP pressate at a pH of 6. The zeta potential of the TMP pressate was within -15 mV and -20 mV, which confirmed that the zeta potential was not affected by the pH adjustment. The results indicated that the increase in the ionic strength of the solution did not have a remarkable effect on the zeta potential of the fly ash/TMP systems.

Impact of the Composition on the Adsorption Parameters

The values of the estimated Freundlich maximum adsorption capacity for lignin adsorption by F1, F2, F3, F4, and F5 were 149 mg/g, 142 mg/g, 143 mg/g, 106 mg/g, and 125 mg/g, respectively, at pH 6. It has been reported previously that the adsorption capacity of activated carbon for lignin from a TMP pressate was 166 mg/g (Oveissi and Fatehi 2014). The adsorption of lignin is expected to occur mostly in the mesopores of the fly ash

(Radovic 2001) because the hydrodynamic diameter of the lignin in the TMP pressate used in this study was 8.5 nm and mesopores have a pore width ranging from 2 nm to 50 nm. As these fly ash samples had a similar surface area and mesopore volumes (Table 4), the adsorption of lignin in these pores could not impact the adsorption capacity of different samples. The zeta potential and ionic strength were not influential on the adsorption of lignin. It is suggested that the chemical composition of fly ash rather than the physical structure of fly ash could have the dominant role in affecting the adsorption capacity.

Figure 4 shows the relationship between the experimentally determined K_F for lignin adsorption, and the total metals, calcium, and potassium contents of the fly ash samples F1 to F5. The results suggested that there was a correlation between the lignin adsorption K_F and the metals content of the fly ash samples (R^2 = 0.981). The metals content of the fly ash consisted of various elements, which made it impossible to determine the effect of specific metals on the adsorption. However, calcium, which represented the largest proportion of the total metals content in the fly ash samples (Table 1), exhibited a linear trend with the lignin adsorption K_F (R^2 = 0.989). The potassium content also related reasonably well to the lignin adsorption K_F (R^2 = 0.965).

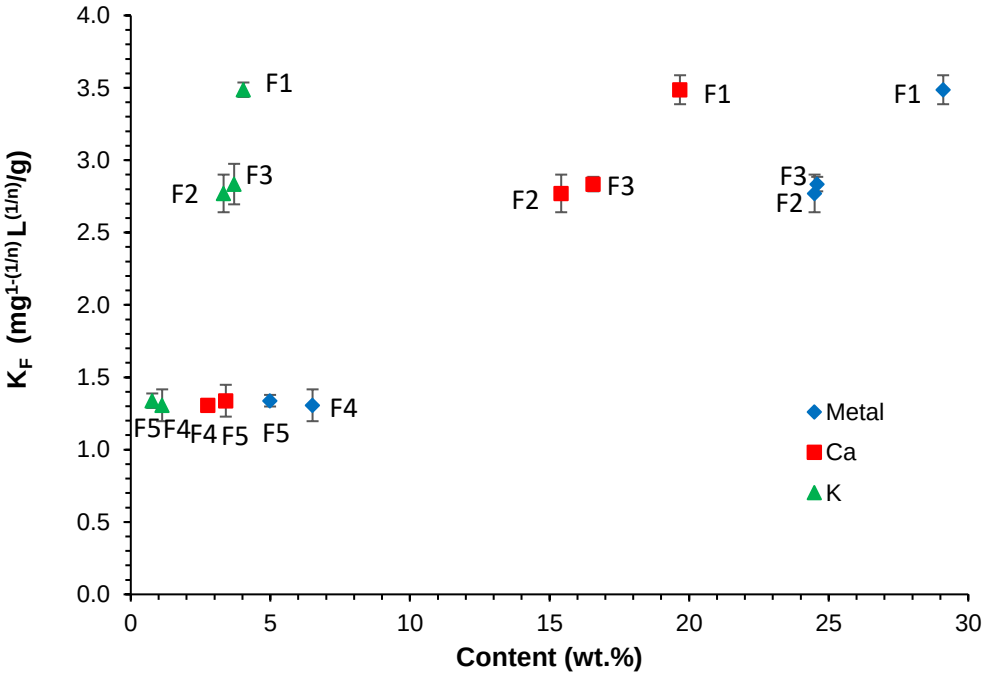

Fig. 4. K_F for the lignin removal as a function of the total metals, calcium, and potassium contents in the biomass-based fly ash; the K_F values for lignin were obtained from the isotherm analysis of F1, F2, F3, F4, and F5

Figure 5 shows the relationship between the K_F for the COD removal from the TMP pressate and the metals, calcium, and potassium contents of fly ash samples F1 through F5. The results indicated that there appeared to be a positive correlation between the COD removal K_F and the metals, calcium, and potassium contents in the fly ash (R^2 values of 0.894, 0.912, and 0.896, respectively).

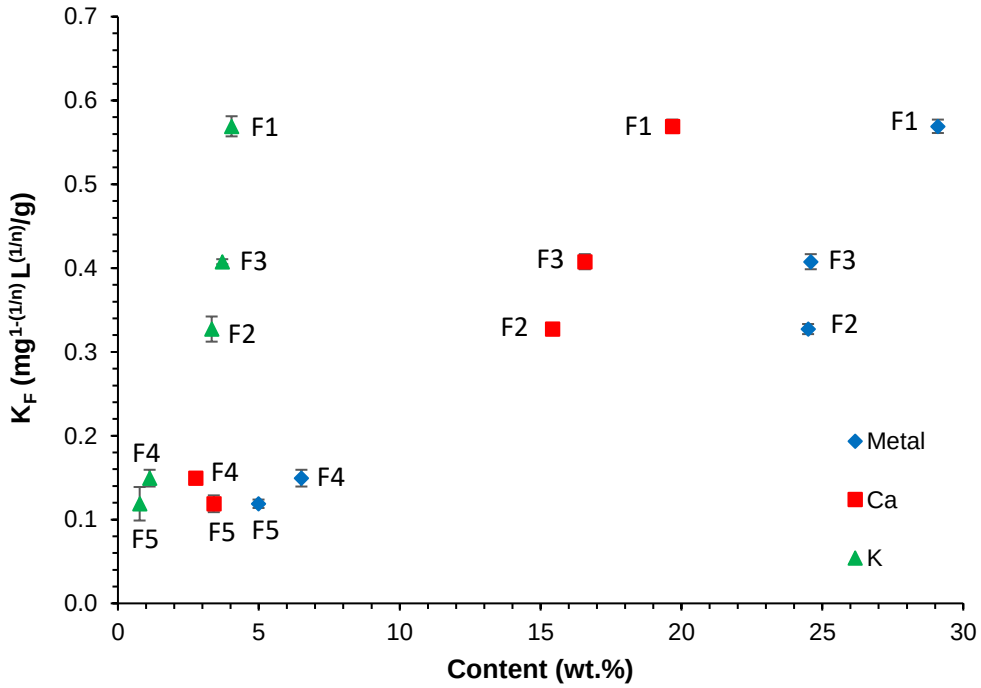

Fig. 5. K_F for the COD removal as a function of the total metals, calcium, and potassium contents in the biomass-based fly ash; the K_F values for COD were obtained from the isotherm analysis of F1, F2, F3, F4, and F5

In Figure 6a, the impact of potassium chloride dosage on the chord length distribution of the TMP pressate is presented. The results indicate that the addition of potassium chloride in the range of 546 to 4567 mg/kg KCl/TMP pressate had no impact on the chord length distribution, implying that potassium chloride did not contribute to coagulation of the components of TMP pressate. Thus, no lignin and COD removals were observed by KCl (data not shown). Figure 6b shows the impact of the calcium chloride dosage on the chord length distribution of the particles in the TMP pressate. The results indicate that as the dosage of calcium chloride increased, the total number of counts and the peak chord length increased suggesting that calcium chloride had a coagulating effect on the constituents in the TMP pressate. In Figure 6c the impact of the calcium chloride dosage on the COD and lignin removals from a TMP pressate are shown. The results indicate that as the dosage of calcium chloride increased from 1040 to 2770 mg/kg $CaCl_2$/TMP pressate, the COD and lignin removals increased from 6.1% to 20.8% and 20.8% to 30.8%, respectively.

Previous studies have reported that lime and precipitated calcium carbonate removed 10% to 16% of lignin from hydrolysis liquor (Saeed *et al.* 2012b; Fatehi *et al.* 2013). Overall, calcium containing compounds have acted as coagulants and improved lignin and COD removals from the TMP pressate. The higher calcium content of the sample was found to contribute to the higher lignin and COD removals (Fig. 6c). Therefore, the reason for the deviation in the results for the fly ash with the largest particle size may be its slightly higher calcium content (3.4%) than that of the other samples (2.5% to 2.8% in Table 2).

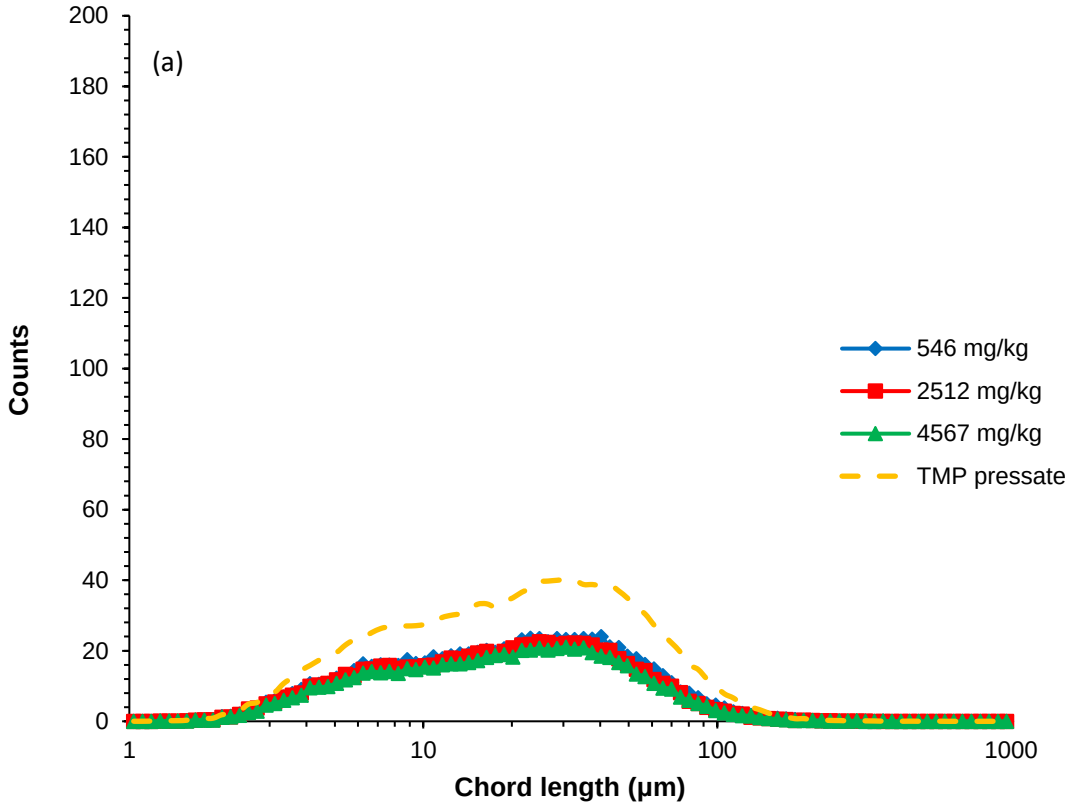
(a)
Counts
Chord length (µm)
546 mg/kg
2512 mg/kg
4567 mg/kg
TMP pressate

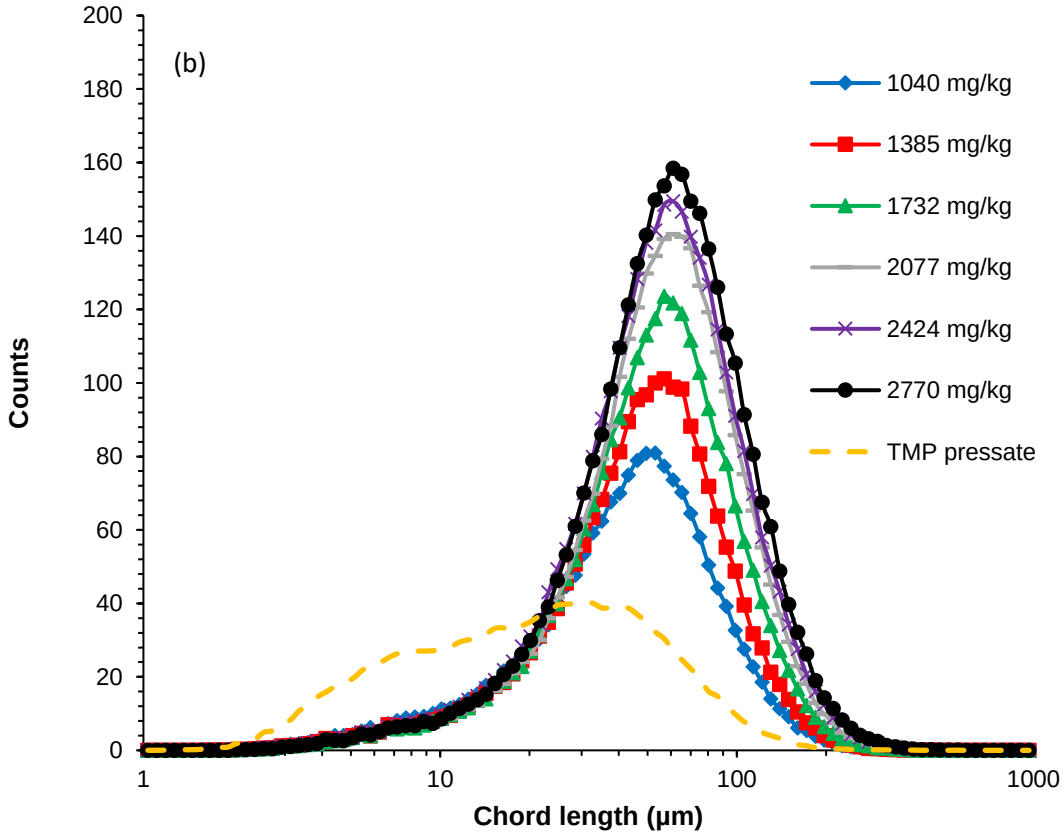
(b)
Counts
Chord length (µm)
1040 mg/kg
1385 mg/kg
1732 mg/kg
2077 mg/kg
2424 mg/kg
2770 mg/kg
TMP pressate

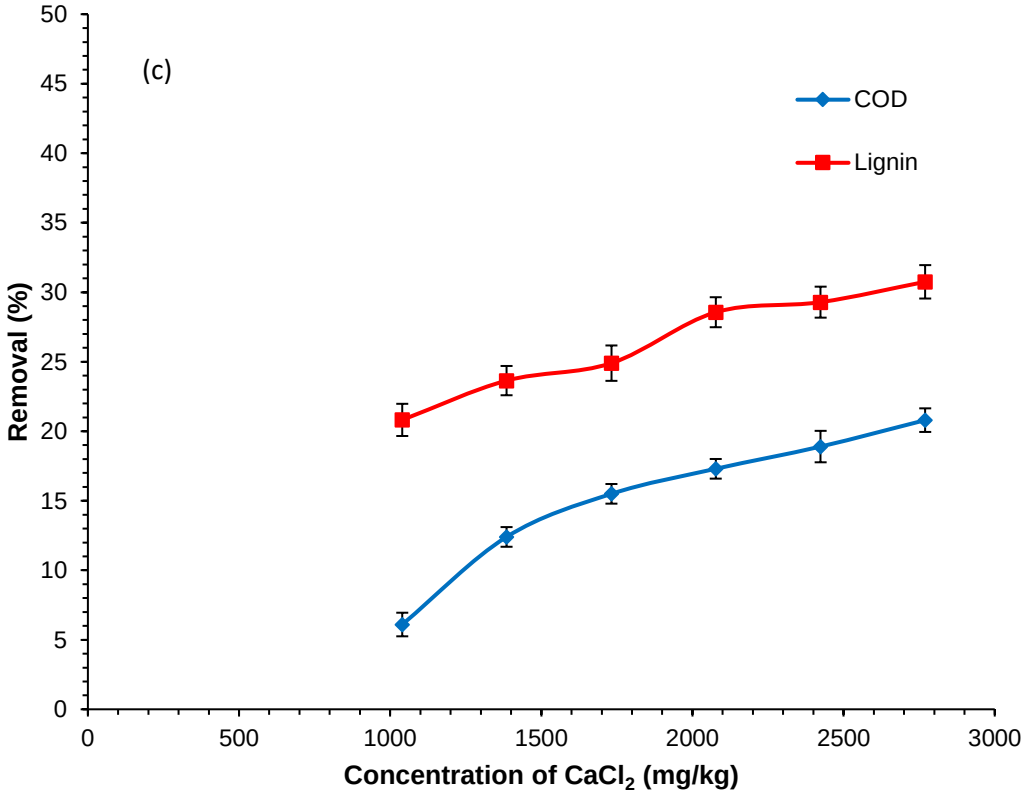

Fig. 6. The impact of potassium chloride dosage (a) and calcium chloride dosage (b) on the chord length distribution of a TMP pressate. (c) The impact of calcium chloride dosage on the COD and lignin removals of a TMP pressate. (Treatment conditions: 200 rpm, pH 12.5, and 298K for 30 min).

Impact of the Particle Size

To determine the impact of the particle size on the lignin and COD removals at a constant fly ash composition, an isotherm analysis was performed on F4, F4S, F4M, and $F_0$4, which had particle size ranges of 0.037 nm to 0.074 mm, 0.105 nm to 0.149 mm, 0.250 nm to 0.297 nm, and 0.420 nm to 0.841 nm, respectively. Figure 7 shows the calculated maximum adsorption capacity of these fly ash samples for the lignin and COD. The estimated Freundlich adsorption capacity for the lignin by F4, F4S, F4M, and $F_0$4 was 270 mg/g, 175 mg/g, 124 mg/g, and 230 mg/g, respectively (Table 4). Furthermore, the estimated Freundlich adsorption capacity for the COD by F4, F4S, F4M, and $F_0$4 was 170 mg/g, 116 mg/g, 64 mg/g, and 103 mg/g, respectively (Table 4). Except for the largest fraction, the results suggested that the lignin and COD removals increased as the particle size of the biomass-based fly ash decreased. As was stated previously, the chemical compositions of the fly ash played an important role in the lignin and COD removals. The higher calcium content of the sample was found to contribute to the higher lignin and COD removals (Fig. 6c). Therefore, the reason for the deviation in the results for the fly ash with the largest particle size may be its slightly higher calcium content (3.4%) than that in the other samples (2.5% to 2.8% in Table 2). Higher adsorption with smaller particle is generally due to the large surface area of particles (Kara *et al.* 2007). However, it is not the case in this study since the surface area of F4, F4S, F4M, and $F_0$4 were different, but they had a similar pore volume (Table 3). This is probably caused by the higher accessibility and availability of adsorption sites on fly ash samples with small particle sizes.

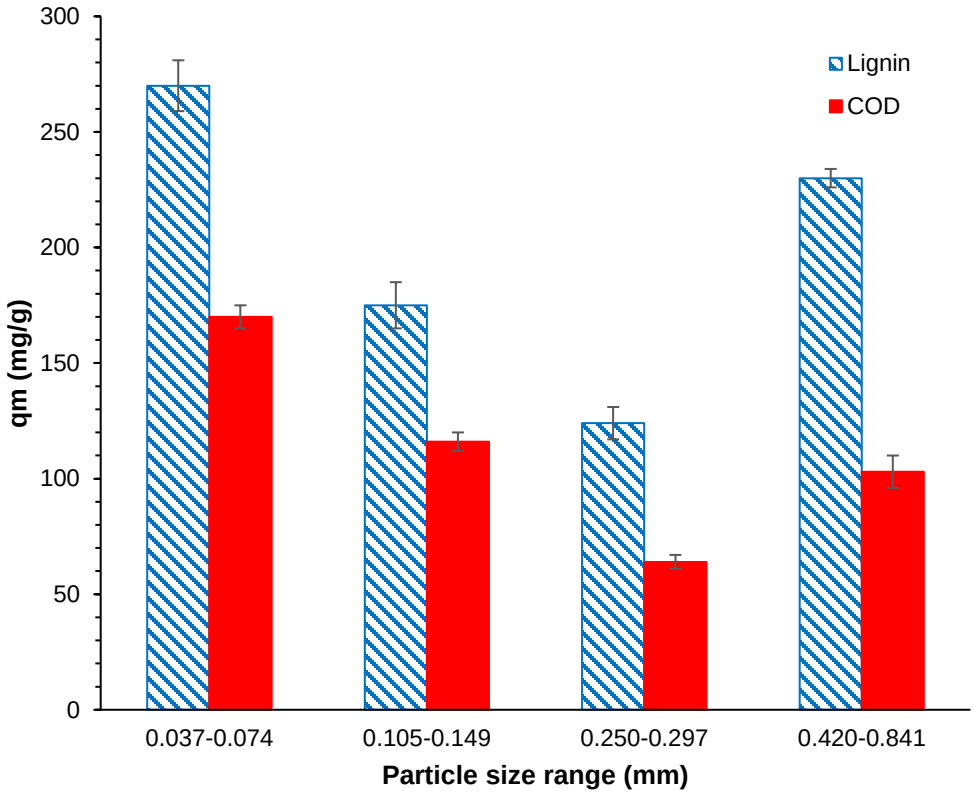

Fig. 7. Comparison of the maximum adsorption capacity and the particle size ranges of the fly ash samples; the fly ash samples were F4, F4S, F4M, and F04, which corresponded to the particle size ranges of 0.037 nm to 0.074 mm, 0.105 nm to 0.149 mm, 0.250 nm to 0.297 nm, and 0.420 nm to 0.841 nm, respectively.

Adsorption Mechanism

The mechanism of lignocellulose adsorption on fly ash was proposed as shown in Fig. 8. When fly ash was added to TMP pressate, the soluble metal components present on fly ash particles dissolved in water, leading to an increase in the pH of the solution and complexion between metals and lignocellulose.

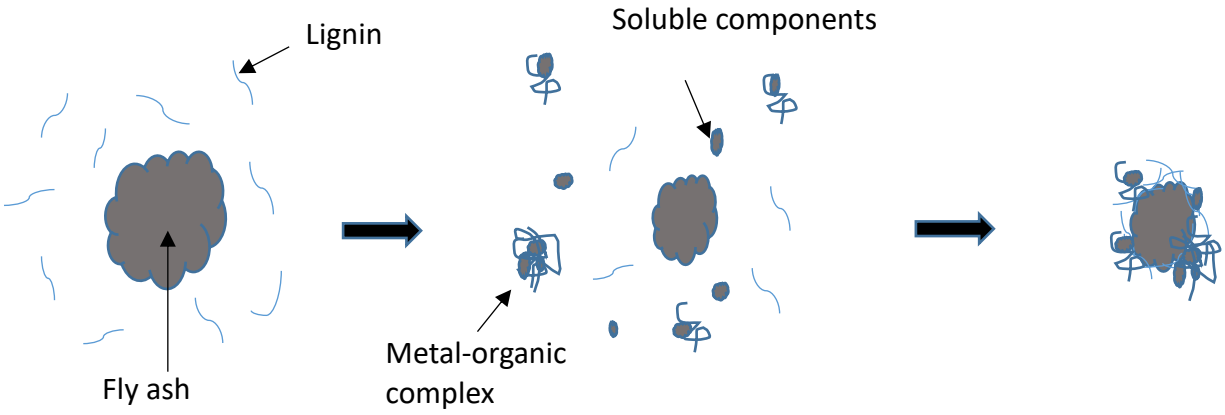

Fig. 8. Proposed mechanism of adsorption of lignin on fly ash

The lignocellulose would be removed by either direct adsorption of lignocellulose onto fly ash surface or the adsorption of formed metal-organic complex. The adjustment of solution pH to acidic could enhance the lignin removal probably due to less solubility of lignin under acidic conditions (due to protonation of carboxylate and phenolate groups). For fly ash with the same particle size, the metal content would significantly contribute to the lignin and COD removals by complexion, while surface area and pore volume would insignificantly impact its adsorption capacity. At a constant elemental composition, fly ash with small particle sizes exhibit higher adsorption capacity than that with large particle sizes.

Practical Applications

The results of this study showed that the particle size and elemental compositions of the fly ash noticeably impacted its adsorption performance. Grinding generally reduced the particle size of the fly ash, but it did not necessarily increase its surface area, as fly ash contained unburned porous biomass, and the mechanical grinding might not substantially increase its surface area. The mechanical grinding might not improve the adsorption capacity of fly ash. The elemental compositions of fly ash can be varied if they are fractionated, as the large fly ash was usually carbonaceous, while the small fly ashes contained inorganic compounds (*i.e.*, metallic compounds). As fractionation impacted the elemental compositions of the fly ash and different elements had different adsorption tendencies, this process might provide a pathway to control the properties of fly ash for achieving the desired adsorption performance. Therefore, fractionation rather than grinding could be used for producing fly ash with the desired properties in terms of small particle size and high metal content as an effective adsorbent for TMP pressate.

CONCLUSIONS

1. It was determined that the COD and lignin removals from a TMP pressate with fractionated fly ash samples followed the Freundlich isotherm models. Under the conditions of 298 K, a pH of 6, 100 rpm, and 24 h, the highest estimated Freundlich adsorption capacity for lignin in the TMP pressate was 149 mg fly ash/g TMP pressate, which was obtained with the fly ash with the highest metals content (29.1 wt.%).
2. The greatest estimated Freundlich adsorption capacity for the COD in the TMP pressate was determined to be 204 mg fly ash/g TMP pressate for fly ash sample F3 under the conditions of 298 K, a pH of 6, 100 rpm, and 24 h. This fly ash had a slightly lower metals content (24.6 wt.%).
3. The results showed that the ionic strength of the fly ash/TMP system did not have a noticeable effect on the adsorption. Furthermore, the metals content of the biomass-based fly ash, specifically potassium and calcium, had a remarkable effect on the K_F values for the lignin and COD adsorption.
4. For the fly ash samples with similar compositions, the particle size had an important impact on the adsorption capacity of the fly ash. Fractionation might be a viable method to produce fly ash with the desired adsorption properties.

ACKNOWLEDGMENTS

The authors would like to thank NSERC-Canada, Canada Foundation for Innovation, Ontario Research Fund, Northern Ontario Heritage Fund Corporation, and Centre for Research and Innovation for Bioeconomy for supporting this research. This paper was prepared based on the MSc work of Germaine Cave at Lakehead University.

REFERENCES CITED

Andersson, K. I., Eriksson, M., and Norgren, M. (2011). "Removal of lignin from wastewater generated by mechanical pulping using activated charcoal and fly ash: Adsorption isotherms and thermodynamics," *Ind. Eng. Chem. Res.* 50(13), 7722-7732. DOI: 10.1021/ie200378s

Andersson, K. I., Eriksson, M., and Norgren, M. (2012). "Lignin removal by adsorption to fly ash in wastewater generated by mechanical pulping," *Ind. Eng. Chem. Res.* 51(8), 3444-3451. DOI: 10.1021/ie202462z

Andersson, K. I., Pranovich, A. V., Norgren, M., Eriksson, M., and Holmbom, B. (2008). "Effects of biological treatment on the chemical structure of dissolved lignin-related substances in effluent from thermomechanical pulping," *Nord Pulp Pap. Res. J.* 23(2), 164-171. DOI: 10.3183/NPPRJ-2008-23-02-p164-171

Abedinzadeh, N., Shariat, M., Monavari, S. M., and Pendashteh, A. (2018). "Evaluation of color and COD removal by Fenton from biologically (SBR) pre-treated pulp and paper wastewater," *Process Saf. Environ. 116*, 82-91. DIO: 10.1016/j.psep.2018.01.015

Cave, G., and Fatehi, P. (2017). "Adsorption optimization of a biomass-based fly ash for treating thermomechanical pulping (TMP) pressate using definitive screening design (DSD)," *Can. J. Chem. Eng.* In press. DOI: 10.1002/cjce.23128

Cretescu, I., Soreanu, G., and Harja, M. (2015). "A low-cost sorbent for removal of copper ions from wastewaters based on sawdust/fly ash mixture," *Int. J. Environ. Sci. Te.* 12(6), 1799-1810. DOI: 10.1007/s13762-014-0596-x

Duan, J., and Gregory, J. (2003). "Coagulation by hydrolysing metal salts," *Adv. Colloid Interface Sci.* 100-102, 475-502. DOI: 10.1016/S0001-8686(02)00067-2

Elliot, A., and Mahmood, T. (2006). "Beneficial uses of pulp and paper boiler ash residues," *Tappi J.* 5(10), 9-16.

Fadeeva, V. P., Tikhova, V. D., and Nikulicheva, O. N. (2008). "Elemental analysis of organic compounds with the use of automated CHNS analyzers," *J. Anal. Chem.+* 63(11), 1094-1106. DOI: 10.1134/S1061934808110142

Fatehi, P., Hamdan, F. C., and Ni, Y. (2013). "Adsorption of lignocelluloses of pre-hydrolysis liquor on calcium carbonate to induce functional filler," *Carbohyd. Polym.* 94(1), 531-538. DOI: 10.1016/j.carbpol.2013.01.081

Fatehi, P., Gao, W., Sun, Y., and Dashtban, M. (2016). "Acidification of prehydrolysis liquor and spent liquor of neutral sulfite semichemical pulping process," *Bioresour. Technol.* 218, 518-525. DOI: 10.1016/j.biortech.2016.06.138

Faust, S. D., and Aly, O. M. (1998). *Chemistry of Water Treatment*, CRC Press LLC, Boca Raton, FL.

Foo, K. Y., and Hameed, B. H. (2010). "Insights into modeling of adsorption isotherm systems," *Chem. Eng. J.* 156(1), 2-10. DOI: 10.1016/j.cej.2009.09.013

Girón, R. P., Ruiz, B., Fuente, E., Gil, R. R., and Suárez-Ruiz, I. (2013). "Properties of fly ash from forest biomass combustion," *Fuel* 114, 71-77. DOI: 10.1016/j.fuel.2012.04.042

Gupta, V. K., Carrott, P. J. M., Carrott, M. M. L. R., and Suhas (2009). "Low-cost adsorbents: Growing approach to wastewater treatment—A review," *Crit. Rev. Env. Sci. Tec.* 39(10), 783-842. DOI: 10.1080/10643380801977610

Gupta, V. K., Ali, I., Saini, V. K. (2007). "Defluoridation of wastewaters using waste carbon slurry," *Water Res.* 41 (15), 3307-3316. DOI: 10.1016/j.watres.2007.04.029

Hamdaoui, O., and Naffrechoux, E. (2007). "Modeling of adsorption isotherms of phenol and chlorophenols onto granular activated carbon: Part I. Two-parameter models and equations allowing determination of thermodynamic parameters," *J. Hazard. Mater.* 147(1-2), 381-394. DOI: 10.1016/j.jhazmat.2007.01.021

Hsieh, C.-T., and Teng, H. (2000). "Influence of mesopore volume and adsorbate size on adsorption capacities of activated carbons in aqueous solutions," *Carbon* 38(6), 863-869. DOI: 10.1016/S0008-6223(99)00180-3

Jaafarzadeh, N., Ghanbari, F., Ahmadi, M., and Omidinasab, M. (2017a). "Efficient integrated processes for pulp and paper wastewater treatment and phytotoxicity reduction: Permanganate, electro-Fenton and Co_3O_4/UV/peroxymonosulfate," *Chem. Eng. J. 308*, 142-150. DOI: 10.1016/j.cej.2016.09.015

Jaafarzadeh, N., Ghanbari, F., and Alvandi, M. (2017b). "Integration of coagulation and electro-activated HSO5− to treat pulp and paper wastewater," *Sustainable Environ. Res. 27* (5), 223-229. DOI: 10.1016/j.serj.2017.06.001

Kao, P.C., Tzeng, J.-H., and Huang, T.-L. (2000). "Removal of chlorophenols from aqueous solution by fly ash," *J. Hazard. Mater.* 76(2-3), 237-249. DOI: 10.1016/S0304-3894(00)00201-6

Kara, S., Aydiner, C., Demirbas, E., Kobya, M., and Dizge, N. (2007). "Modeling the effects of adsorbent dose and particle size on the adsorption of reactive textile dyes by fly ash," *Desalination* 212 (1), 282-293. DOI: 10.1016/j.desal.2006.09.022

Kamali, M., and Khodaparast, Z. (2015). "Review on recent developments on pulp and paper mill wastewater treatment," *Ecotox. Environ. Safe.* 114, 326-342. DOI: 10.1016/j.ecoenv.2014.05.005

Lanzerstorfer, C. (2015). "Investigation of the contamination of a fly ash sample during sample preparation by air classification," *Int. J. Environ. Sci. Te.* 12(4), 1437-1442. DOI: 10.1007/s13762-014-0586-z

Li, W., Wang, Q., Cui, S. W., Huang, X., and Kakuda, Y. (2006). "Elimination of aggregates of (1→3) (1→4)-β-D-glucan in dilute solutions for light scattering and size exclusion chromatography study," *Food Hydrocolloid.* 20(2), 361-368. DOI: 10.1016/j.foodhyd.2005.03.018

Liu, Z., Fatehi, P., Jahan, M. S., and Ni, Y. (2011). "Separation of lignocellulosic materials by combined processes of pre-hydrolysis and ethanol extraction," *Bioresour. Technol.* 102(2), 1264-1269. DOI: 10.1016/j.biortech.2010.08.049

Mall, I. D., Srivastava, V. C., Agarwal, N. K., and Mishra, I. M. (2005). "Adsorptive removal of malachite green dye from aqueous solution by bagasse fly ash and activated carbon-kinetic study and equilibrium isotherm analyses," *Colloids Surf. A Physicochem. Eng. Asp. 264* (1-3), 17-28. DOI: 10.1016/j.colsurfa.2005.03.027

Oveissi, F., and Fatehi, P. (2014). "Isolating lignin from spent liquor of thermomechanical pulping process *via* adsorption," *Environ. Technol.* 35(20), 2597-2603. DOI: 10.1080/09593330.2014.913692

Oveissi, F., and Fatehi, P. (2015a). "Process for treating spent liquor of the TMP process with biomass-based fly ash," *Ind. Eng. Chem. Res.* 54(29), 7301-7308. DOI: 10.1021/acs.iecr.5b01473

Oveissi, F., and Fatehi, P. (2015b). "Characterization of four different lignin as a first step toward the identification of suitable end-use applications," *J. Appl. Polym. Sci.* 132(32), 42336. DOI: 10.1002/app.42336

Pérez, M., Torrades, F., Domènech, X., and Peral, J. (2002). "Removal of organic contaminants in paper pulp effluents by AOPs: An economic study," *J. Chem. Technol. Biotechnol.* 77 (5), 525-532. DOI: 10.1002/jctb.610

Pokhrel, D., and Viraraghavan, T. (2004). "Treatment of pulp and paper mill wastewater—A review," *Sci. Total Environ.* 333(1-3), 37-58. DOI: 10.1016/j.scitotenv.2004.05.017

Radovic, L. R. (2001). *Chemistry of Physics of Carbon*, Marcel Dekker, New York, NY.

Rajamma, R., Ball, R. J., Tarelho, L. A. C., Allen, G. C., Labrincha, J. A., and Ferreira, V. M. (2009). "Characterisation and use of biomass fly ash in cement-based materials," *J. Hazard. Mater*. 172 (2), 1049-1060. DOI: 10.1016/j.jhazmat.2009.07.109

Saeed, A., Jahan, M. S., Li, H., Liu, Z., Ni, Y., and van Heiningen, A. (2012a). "Mass balances of components dissolved in the pre-hydrolysis liquor of kraft-based dissolving pulp production process from Canadian hardwoods," *Biomass Bioenerg.* 39, 14-19. DOI: 10.1016/j.biombioe.2010.08.039

Saeed, A., Fatehi, P., and Ni, Y. (2012b). "An integrated process for removing the inhibitors of the prehydrolysis liquor of kraft-based dissolving pulp process *via* cationic polymer treatment," *Biotechnol. Progr.* 28(4), 998-1004. DOI: 10.1002/btpr.1563

Scherdel, C., Reichenauer, G., and Wiener, M. (2010). "Relationship between pore volumes and surface areas derived from the evaluation of N_2-sorption data by DR-, BET- and t-plot," *Micropor. Mesopor. Mat.* 132(3), 572-575. DOI: 10.1016/j.micromeso.2010.03.034

Singh, A., and Prasad, S. M. (2015). "Remediation of heavy metal contaminated ecosystem: An overview on technology advancement," *Int. J. Environ. Sci. Te.* 12(1), 353-366. DOI: 10.1007/s13762-014-0542-y

Sixta, H. (2006). *Handbook of Pulp*, Wiley-VCH Verlag GmbH and Co. KGaA, Weinheim, Germany.

Sumathi, S., and Hung, Y.-T. (2004). "Treatment of pulp and paper mill wastes," in: *Handbook of Industrial and Hazardous Wastes Treatment*, L. K. Wang, Y.-T. Hung, H. H. Lo, and C. Yapijakis (eds.), CRC Press, Boca Raton, FL, pp. 469-513.

Thompson, G., Swain, J., Kay, M., and Forster, C. F. (2001). "The treatment of pulp and paper mill effluent: A review," *Bioresour. Technol.* 77(3), 275-286. DOI: 10.1016/S0960-8524(00)00060-2

Ugurlu, M., Gurses, A., Yalcin, M., and Dogar. (2005). "Removal of phenolic and lignin compounds from bleached Kraft mill effluent by fly ash and sepiolite," *Adsorption* 11, 87-97. DOI: 10.1007/s10450-005-1096-6

Wang, S., Boyjoo, Y., Choueib, A., Ng, E., Wu, H., and Zhu, Z. (2005). "Role of unburnt carbon in adsorption of dyes on fly ash," *J. Chem. Technol. Biot*. 80(10), 1204-1209. DOI: 10.1002/jctb.1299

Wang, S., and Wu, H. (2006). "Environmental-benign utilisation of fly ash as low-cost adsorbents," *J. Hazard. Mater.* 136(3), 482-501. DOI: 10.1016/j.jhazmat.2006.01.067

Yang, K., Peng, J., Srinivasakannan, C., Zhang, L., Xia, H., and Duan, X. (2010). "Preparation of high surface area activated carbon from coconut shells using microwave heating," *Bioresour. Technol.* 101(15), 6163-6169. DOI: 10.1016/j.biortech.2010.03.001

Zasadowski, D., Yang, J., Edlund, H., and Norgren, M. (2014). "Antisolvent precipitation of water-soluble hemicelluloses from TMP process water," *Carbohyd. Polym.* 113, 411-419. DOI: 10.1016/j.carbpol.2014.07.033

Zheng, M., and Liao, B. Q. (2014). "A comparative study on thermomechanical pulping pressate treatment using thermophilic and mesophilic sequencing batch reactors," *Environ. Technol.* 35(11), 1409-1417. DOI: 10.1080/09593330.2013.869623

Zhu, Z., Wang, X., Dai, S., Huang, B., and He, Q. (2013). "Fractional characteristics of coal fly ash for beneficial use," *J. Mater. Civil Eng.* 25(1), 63-69. DOI: 10.1061/(ASCE)MT.1943-5533.0000550

Article submitted: April 12, 2018; Peer review completed: June 28, 2018; Revised version received: October 11, 2018; Accepted: October 20, 2018; Published: October 29, 2018.
DOI: 10.15376/biores.13.4.9092-9115